JOURNAL OF MECHANICAL ENGINEERING AND SCIENCES
ISSN: 2289-4659 e-ISSN: 2231-8380
VOLUME 19, ISSUE 2, 2025, 10631 - 10641
DOI: https://doi.org/10.15282/jmes.19.2.2025.5.0834

RESEARCH ARTICLE

Fluid-structure coupling effect on the setting process of expansive downhole emergency packer

L. Zhou[1], W. Song[2], H. Liu[1], X. Huang[1]*

[1] College of Pipeline and Civil Engineering, China University of Petroleum, Qingdao 266580, Shandong, China
Phone: +86 18765926339, Fax.: +86 532 86981774

[2] CNPC Research Institute of Safety & Environment Technology, Beijing 102206, China

ABSTRACT - A downhole emergency packer is prepared to seal the drill pipe-casing annulus when the high-pressure overflow and kicks occur during offshore drilling. When there exists fluid in the annulus, the increase in fluid pressure during setting increases the difficulty of working and even results in sealing failure. The primary objective of this research is to investigate the influence mechanism of downhole fluid on the setting efficiency, and provide theoretical support for solving such problems under hydrodynamic conditions. In this work, the hyperelastic constitutive model of the rubber cylinder was established through uniaxial tension and uniaxial compression tests. The fluid-structure coupling model was developed by finite element method, to simulate the setting process of the downhole emergency packer and quantitatively evaluate the impact of downhole fluids on setting efficacy. The results revealed that the fluid velocity and pressure increased throughout the setting process while the annular area shrank, raising the setting difficulty. The existence of fluid flow considerably diminished the setting efficacy of the rubber cylinders. The sealing coefficient, *K* decreased by 7.15%, 11.06%, and 14.41% when the flow velocities from the inlet were 5 m/s, 6 m/s, and 7 m/s, respectively. Therefore, the setting pressure could be increased according to the actual downhole conditions to achieve the actual setting effect safely.

ARTICLE HISTORY
Received : 30th July 2024
Revised : 20th Feb. 2025
Accepted : 02nd May 2025
Published : 30th June 2025

KEYWORDS
Emergency
Downhole packer
Fluid-solid coupling
Sealing property
Flow velocity

1. INTRODUCTION

The geological conditions for offshore exploratory well drilling are generally complicated, which raises the possible incidence of high-pressure overflow and kicks. As high-pressure overflow or well kicks occur at the bottom of the well, the high-pressure overflow penetrates the wellbore annulus presently. It induces an excessively high pressure in the annulus, hence complicating the well-killing procedure and increasing the risk of well-control [1]. Downhole emergency packers are ideal control instruments used underground to avert well kicks and high-pressure overflow from propagating to the wellhead. The emergency packer may efficiently seal the drill pipe-casing annulus and obstruct high-pressure fluid at the bottom of the well, providing enough time for emergency reaction on the platform [2].

The rubber cylinder is important for downhole emergency packers because it primarily executes the sealing process. The nitrile–butadiene rubber (NBR) is used to produce the rubber cylinder due to its excellent mechanical qualities under significant deformations. The assessment of the sealing properties depends critically on the deformation and contact stress during the sealing process. How to choose an appropriate constitutive model to describe the mechanical behavior of the rubber cylinder is very concerning to petroleum engineers. There are a lot of constitutive models for rubber, including the Mooney-Rivlin [3,4], Yeoh [5], Ogden [6], and Gent [7] models, and various constitutive models for rubber exhibit suitability for distinct types of rubber materials [8, 9]. The reasonable selection of the rubber constitutive model directly affects the design success and credibility of the results, and it becomes more crucial, especially in structural design and optimization using the analysis of finite elements. Shim et al. [10] analyzed the strain rate-dependent mechanical characteristics of different rubbers using Hopkinson experiments and established a viscoelastic constitutive theory to describe the tension and compression features of the packer rubber. Liu et al. [11] analyzed the failure mechanism of the compression rubber and found that excessive stress led to compression and fatigue failure of the upper rubber cylinder. Zheng et al. [12] established a contact pressure calculation model to assess the sealing effect of packer. Liu et al. [13] proposed a comprehensive sealing performance evaluation system for packer rubber cartridges. Fan et al. [14] carried out theoretical calculations and experimental testing on the sealing performance of the retrievable packer sealing structure. Kang [15] established a mathematical model of the deformation process of the packer rubber barrel considering the contact nonlinearity during the setting process of the packer and optimized the shoulder structure. Liu et al. [16] developed a finite element (FE) model of a compressed packer rubber cylinder and then examined the influence of the height, thickness, and external angles of the rubber cylinders on the setting effect. Zhang et al. [17] performed experimental tests of the mechanical characteristics of packer rubber cylinders at various temperatures by applying non-contact optical measuring techniques to quantify the deformations of the rubber samples. Zheng and Li [18] analyzed the effects of temperature and stress relaxation on the sealing system of a rubber packer by combining stress relaxation experiments

***CORRESPONDING AUTHOR | X. G. Huang** | ✉ huangxg@upc.edu.cn

and tensile experiments of hydrogenated nitrile rubber (HNBR) at various temperatures. Ben and Jens [19] measured the constitutive models of HNBR exposed in an oil well at extreme pressure and temperature. Dong and Li [20] evaluated the constitutive model characteristics of rubber seals using heat degradation experiments and developed a FEM calculation model for the static condition of the packer. Jin et al. [21] tested the sealing properties of HNBR and a fluoroelastomer rubber (AFLAS) materials used in high-temperature packers and discussed the impact of temperature on the setting performance.

The setting of a downhole emergency packer is a process of blocking high-pressure fluid. Therefore, the influence of high-pressure fluid during the setting process of emergency packers cannot be ignored. Bruman et al. [22] established a contact model with fluid-solid interaction, which provided a method for fluid-solid coupling of packer rubber. Wu and Li [23] analyzed the setting performance of rubber cylinders in high hydraulic environments and obtained the fluid pressure distribution and rubber contact pressure distribution in fluid-structure coupling environments. Salant and Yang [24] established an elastohydrodynamic lubrication model to simulate the performance of a hydraulic seal. Wen et al. [25] established a lip seal fluid-solid coupling model to reveal the complex coupling effect between fluid and rubber deformation. Yao et al. [26] proposed a thermal fluid–solid interaction mechanism and dynamic response (TFSID) model to study the fluid-solid coupling effect in a mechanical seal. Xiang et al. [27] and Wei et al. [28] analyzed the rubber sealing process under fluid-solid interaction and the contact pressure distribution under different working conditions. Angerhausen et al. [29] optimized the rubber structure in mechanical seals by studying the flow field and deformation of hyperelastic rubber.

At present, constitutive models for rubber materials at different temperatures and the structural design of rubber packers are available. Nevertheless, the mentioned research mainly focuses on the deformation and tension of the packer under a single action of setting pressure, and the coupling or interaction between the fluid and rubber cylinder is always ignored. In reality, the setting of the downhole emergency packer is a dynamic process in the annulus filled with high-speed and high-pressure fluid. The action of high-pressure and high-velocity fluid on the rubber cylinder may cause changes in sealing properties, such as contact stress and contact width, thereby altering the overall sealing efficacy and resulting in the setting failure. Therefore, in this work, a fluid-structure coupling model for the rubber cylinder of the emergency packer was established to simulate the whole setting process of high-pressure fluid. The effects of fluid pressure and velocity on the setting performance were evaluated.

2. MATERIAL AND METHODS

2.1 The Structure of the Downhole Emergency Packer

Figure 1 illustrates the configuration of the downhole emergency packer. The packer primarily contains a central pipe, an unidirectional valve, and an interior/exterior rubber cylinder. When an abnormal annular pressure is detected, the downhole emergency packer can be placed at a specific distance below the wellhead through the drill pipe. Once the emergency packer is in place, the setting fluid is pressurized into the internal flow channel inside the central pipe. When the fluid pressure approaches a certain value, the fluid can enter the space between the rubber cylinder and the central tube through the inlet hole. The fluid pressure in the gap continuously increased, squeezing rubber outward to seal the packer-casing area, depicted in Figure 2.

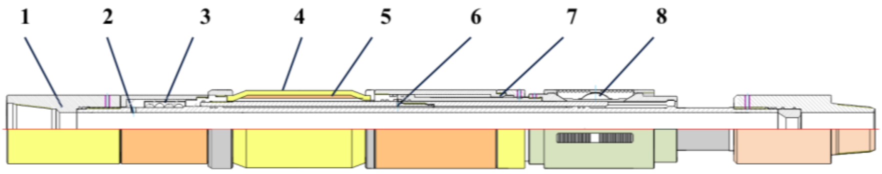

Figure 1. The structure of the downhole emergency packer (1- central pipe; 2- inlet hole; 3- unidirectional valve; 4- exterior rubber cylinder; 5- interior rubber cylinder; 6-pressure relief hole; 7-slip; 8-self-locking structure)

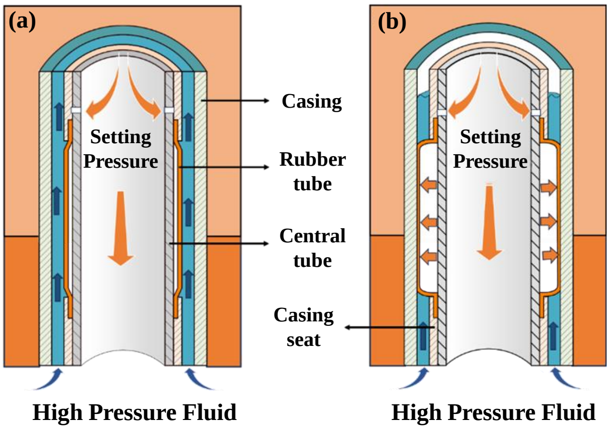

Figure 2. Working process of the emergency packer: (a) starting sealing and (b) sealing completed

2.2 Constitutive Model of Nitrile–Butadiene Rubber

The mechanical properties of the rubber cylinder determine the sealing performance of the downhole emergency packer. The rubber cylinder is made of NBR whose stress-strain relationship is nonlinear. The hyperelastic constitutive model is used to describe the mechanical behavior of the packer cylinder. Assuming complete hyperelasticity of packer rubber, its mechanical behavior can be described by the strain energy density function, *W*, and different strain energy density functions, *W* are suitable for different materials. In this paper, *W* proposed by Mooney and Rivlin is used to describe the mechanical behavior of rubber cylinders. As shown in Eq. (1), this model can be well applied to packer rubber material [30].

$$W = C_{01}(I_1 - 3) + C_{10}(I_2 - 3) + \frac{1}{D_1}(J - 1)^2 \tag{1}$$

where, J is the volume ratio before and after deformation, C_{01} and C_{10} are the superelasticity coefficients, D_1 is the compressibility coefficient, and I_1 and I_2 are the first and second strain invariants, respectively.

To determine its constitutive model, uniaxial compression and tensile tests were performed by the GB/T 7757-2009 and GB/T 528-2009 [31]. The material was tested using the ETM105D universal testing machine. The tensile and compression rates were set to 500 mm/min and 10 mm/min respectively to ensure the quasistatic loading. The uniaxial tension and compression experiments, together with the dimensions of the testing samples, are shown in Figure 3, every test run three times to ensure the accurate results. Figure 4 illustrates the tensile and compressive stress-strain curves of the NBR. Based on the test results, the fitted material constants for the Mooney-Rivlin model are the following: $C_{10} = 1.87244$, $C_{01} = 0.9531$.

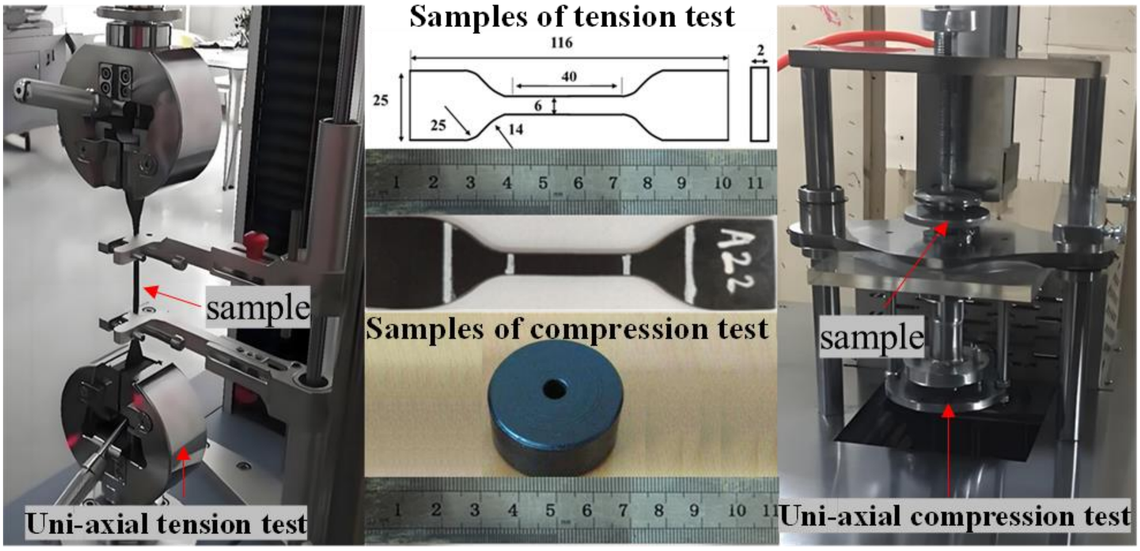

Figure 3. The uni-axial tension and compression test setup

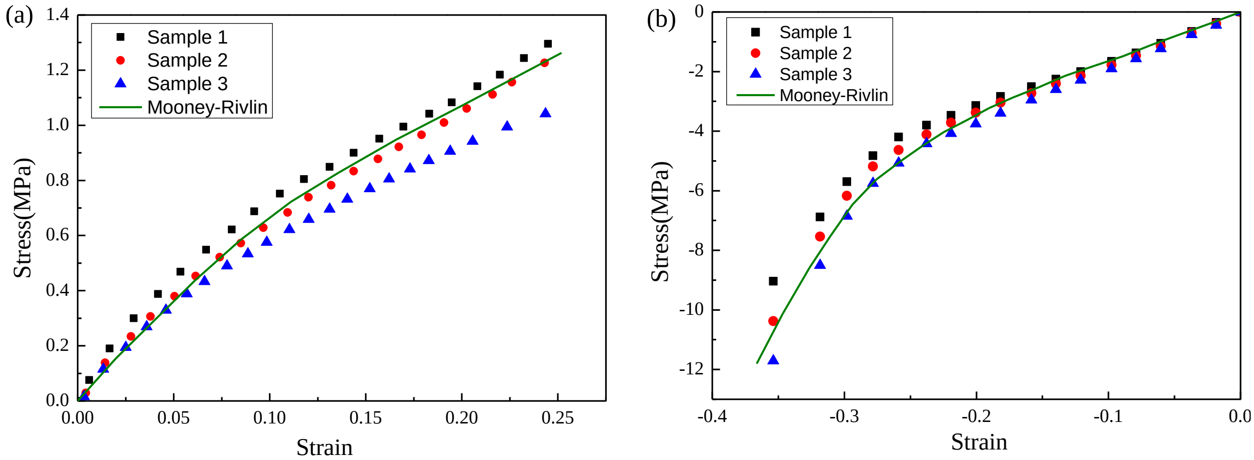

Figure 4. Fit curves between the stress-strain data obtained from the tests and the Money-Rivlin constitutive model of the NBR: (a) tension and (b) compression

2.3 Fluid-Structure Method

To evaluate the sealing efficacy of downhole emergency packers in real downhole conditions, it is essential to account for the impact of downhole fluid on the deformation of the rubber tube. Assuming the annulus fluid is viscous, incompressible and Newtonian, it satisfies the Navier-Stokes equations and the continuity equation [32,33],

$$\frac{\partial\rho}{\partial t} + \nabla.(\rho\mathbf{V}) = 0 \tag{2}$$

$$\rho\frac{\mathrm{d}\mathbf{V}}{\mathrm{d}t} = \rho\mathbf{F} - \nabla p + \mu\nabla\mathbf{V} = 0 \tag{3}$$

where, $\mathbf{V}$ is the fluid velocity vector, ρ is the density of the fluid, μ is the fluid viscosity coefficient, $\mathbf{F}$ is the stress tensor, and p is the pressure.

The equation of motion for a solid without considering mass forces can be written as:

$$\rho_s\mathbf{a}_s = \nabla.\boldsymbol{\sigma}_s \tag{4}$$

where, ρ_s is the density of the solid, $\mathbf{a}_s$ is the acceleration vector of the solid, and $\boldsymbol{\sigma}_s$is the stress tensor of the solid.

The solid control equation for solid stress and deformation caused by fluid is:

$$M_s\ddot{\mathbf{d}}_s + C_s\dot{\mathbf{d}}_s + K_s\mathbf{d}_s = \boldsymbol{\tau}_s \tag{5}$$

where, M_s is the solid mass matrix, C_s is the damping matrix, K_s is the solid stiffness matrix, $\mathbf{d}_s$is the solid displacement vector, and $\boldsymbol{\tau}_s$is the load vector of the solid.

Fluid-structure coupling follows the basic principle of conservation. Therefore, the treatment of the fluid-structure coupling interface is very important for fluid-structure coupling. Through the coupling interface, the fluid flow affects the solid motion, which in turn affects the flow field. The velocity, displacement and force between the overflow fluid and rubber cylinder can be transmitted through the interface. Therefore, the fluid-structure coupling interface between the fluid and the rubber cylinder satisfies the following equations [34],

$$\mathbf{d}_f = \mathbf{d}_s \tag{6}$$

$$\boldsymbol{\tau}_f.\mathbf{n}_f = \boldsymbol{\tau}_s.\mathbf{n}_s \tag{7}$$

where, $\mathbf{d}$, $\boldsymbol{\tau}$ and $\mathbf{n}$ represent the displacement, load, and boundary normal direction vectors, respectively, and the subscripts f and s represent the fluid on the outer wall of the rubber cylinder and the fluid in the packer, respectively.

As mentioned above, the sealing procedure of the emergency packer is a strong fluid-structure coupling (FSC) process. The bidirectional FSC model was established to achieve good simulation results. The FSC model is divided into solid and fluid domains, in which the fluid domain calculates the fluid velocity and pressure, and the solid domain calculates the deformation and stress and transmits the displacement deformation to the fluid domain through the coupling surface [35]. The emergency packer sealing process was simulated using ANSYS and FLUENT. First, the initial fluid and solid fields were imported into ANSYS and FLUENT, respectively. The fluid field is calculated to extract the pressure of the fluid field after reaching a steady state, and the fluid-structure interaction surface is imported into ANSYS. Then, the solid domain in ANSYS undergoes deformation under fluid pressure, and the fluid field is reconstructed according to the extracted solid deformation. The fluid field is imported into FLUENT to obtain the fluid pressure. Finally, the FSC calculation process is repeated until the calculation convergence of the solid domain.

2.4 Finite Element Model

The primary technical details of the packer are as follows: setting pressure 10 MPa to seal an annulus between the 9 ⅝ " casing and 5" drill pipe, the inner and outer diameters of the rubber cylinder are 148 mm and 198 mm, respectively. The casing, drill pipe, and rubber cylinder seats are made of high-quality alloy steel (42CrMn) with a Poisson's ratio of 0.28 and an elastic modulus of 210 GPa. Figure 5 shows the axisymmetric fluid-structure model of the emergency packer. Figure 5(a) shows the physical model for fluid-solid coupling analysis of the emergency packer, in which the casing is 1200 mm long, the middle part is 500 mm long, and the outer diameter of annular fluid domain, D is 238mm. To fully develop the flow in the annular fluid domain, the length of the fluid domain is 1200 mm (greater than 5d). Figure 5(b) shows the solid and fluid domains in the finite element model. Because the model is axisymmetric, the axisymmetric model is used for finite element analysis in both solid and fluid domains.

The transient analysis is adopted in the fluid-solid coupling analysis of the packer. The boundaries of each part of the solid domain are symmetrically constrained. A 12MPa pressure is applied to the inner side of the rubber cylinder as the setting pressure. The fluid-solid coupling interface is adopted on the outer surface of the rubber cylinder, through which the pressure generated during fluid flow can transmit. The k-epsilon (k - ε) turbulence model is used to analyze the fluid domain. This model can fully describe the fluid flow in the narrow annulus of the packer. The initial conditions, i.e., the velocity inlet and pressure outlet are set as 5 m/s and 10 MPa, respectively, according to the actual application. In finite element simulations, mesh refinement can obtain accurate solutions but increase computational costs. Therefore, verifying mesh independence is of great significance for the accuracy of the results. By changing the overall mesh density of the solid and fluid domains, the mesh independence of the maximum contact stress in the solid domain under fluid-solid coupling was verified, as shown in Figure 6. It can be seen that mesh refinement does not significantly increase accuracy, but the computational cost greatly increases when the overall mesh size is refined to 4 mm. Therefore, the case of dividing the overall mesh into 4mm was ultimately selected as the finite element model mesh. According to the mesh independence of the maximum contact stress in the solid domain, the final mesh size of 4 mm was determined by balancing efficiency and accuracy.

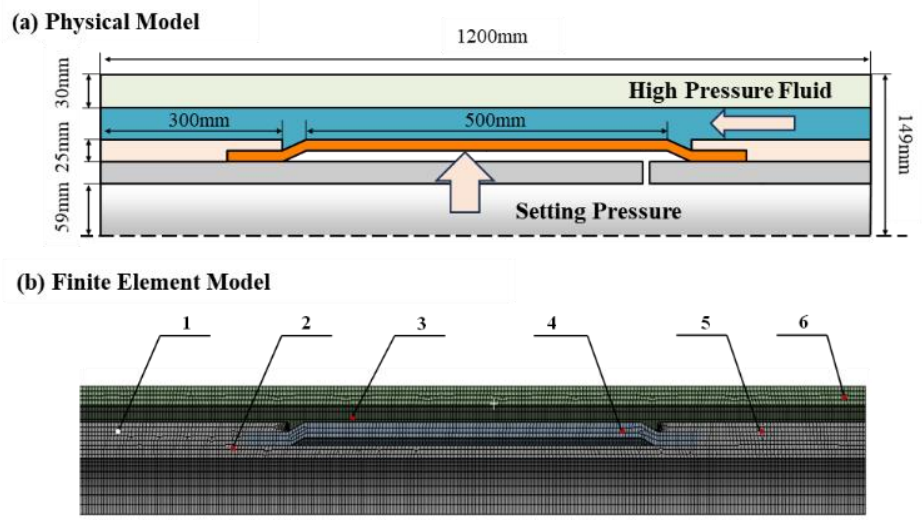

Figure 5. Axisymmetric model of fluid-structure coupling for emergency packer: (a) Physical model, (b) Solid and fluid domain (1-upper rubber cylinder seat; 2-central pipe; 3-fluid in the annulus; 4-rubber cylinder; 5-drill pipe wall; 6-casing pipe wall)

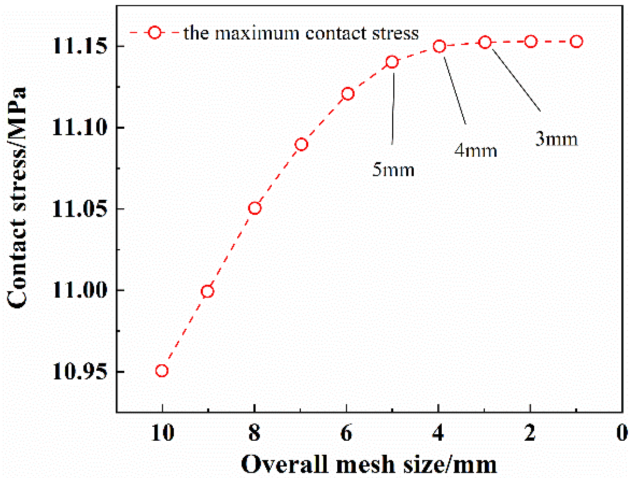

Figure 6. The verification of mesh independence in the finite element simulation

3. RESULTS AND DISCUSSION

3.1 Setting Performance of the Emergency Packer

Figure 7 illustrates the variation curves of contact stress and Mises stress for the central unit of the rubber cylinder. Three phases may be distinguished in the setting process: the extraction stage OA (0-5 seconds), the contact deformation stage OB (5-12 seconds), and the setting completion stage OC (12-20 seconds). At the beginning of the sealing process, the pressure differential between the interior and exterior surfaces causes the rubber cylinder to expand and deform. At this time, the rubber cylinder is compressed, resulting in changes in the shape of the fluid domain and fluid pressure. At the stage of rubber cylinder compression, the effect of fluid pressure on the rubber deformation is gradually emerging. When setting pressure increases, the rubber cylinder continues to expand, and the high-pressure fluid is prevented from surging along the annulus towards the wellhead. The contact area and stress between the rubber cylinder and the casing continue to increase until the setting is completed. At this time, the contact area and stress reach their maximum values, and the rubber cylinder enters a fully seated state. In this condition, the rubber cylinder obstructs the gap between the drilling tube and casing, preventing high-pressure oil and gas from rushing toward the wellhead via the annulus.

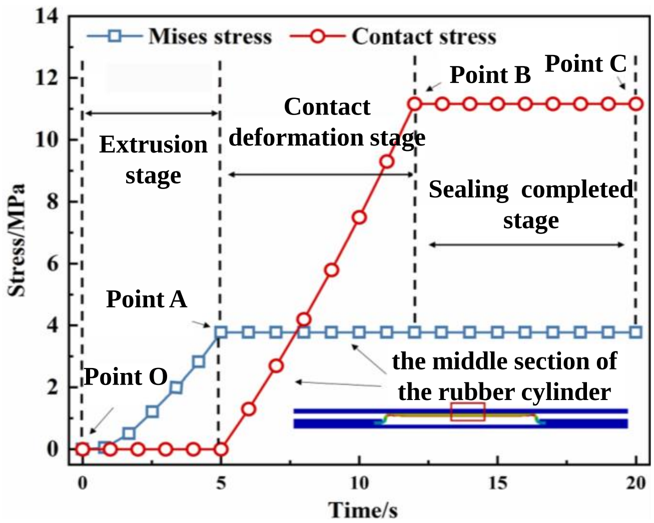

Figure 7. Contact stress and Mises stress variation of the rubber cylinder at each stage

Figure 8 demonstrates the displacement and Mises stress of the rubber cylinder at different stages of the setting procedure. In the first 5 seconds, the rubber cylinder remains in the first deformation phase and the displacement change during this stage is mainly concentrated on the middle section. As time goes on, the rubber cylinder's maximum displacement slowly moves up. This is because of the uneven pressure exerted by the fluid on the rubber cylinder owing to changes in the fluid domain. After 5 seconds, the rubber cylinder enters the contact deformation stage, and the initial contact area lies in the upper-middle section.

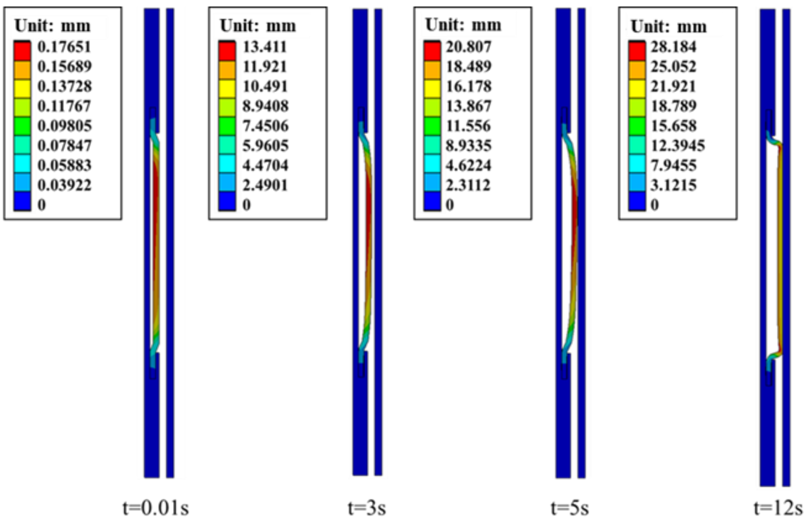

(a) displacement

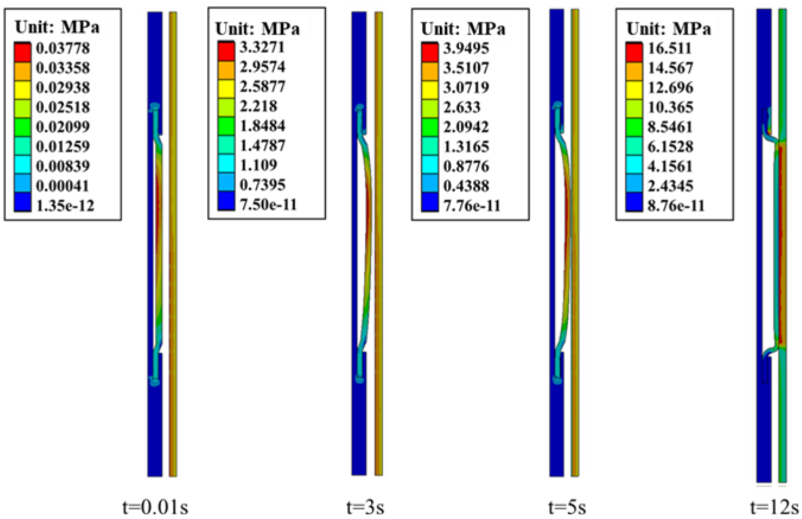

(b) von Mises stress

Figure 8. The displacement and stress distribution during the setting process: (a) displacement and (b) von-Mises stress

The rubber cylinder enters the sealing completion stage when the setting time exceeds 12 seconds. The rubber cylinder is closely attached to the casing wall, and the fluid is sealed. In the extrusion stage, the maximum Mises is always in the middle section without touching the casing. Then, the maximum stress gradually moves towards the upper middle section, which is similar to the maximum displacement. When the setting is complete, as the packer rubber and the casing are compressed against each other, the maximum Mises stress is transferred to the center of the casing.

Figure 9 shows the displacement and Mises stress along a specific path in the rubber cylinder for different setting times. From 0 to 5 seconds, the maximum displacement is observed in the central part, and the maximum displacement gradually moves towards the upper middle section. When t = 5 seconds, the Maximum outside rubber cylinder displacement is 19.8 mm. At this time, the rubber cylinder contacts the casing and enters the contact-deformation stage. When the rubber cylinder is seated, the maximum displacement appears at both ends, and the displacement curve exhibits a "bull horn" shape. Similar to the displacement distribution, the maximum Mises stress gradually moves towards the upper middle section over time. The maximum Mises stress reaches 3.8 MPa in the middle section at t = 5 seconds, and it increases to 12.9 MPa at t = 12 seconds. The maximum Mises stress occurs at the positions of 100-150 mm and 650-700 mm on both sides. Therefore, appropriate protective measures are recommended at these positions to reduce working stress.

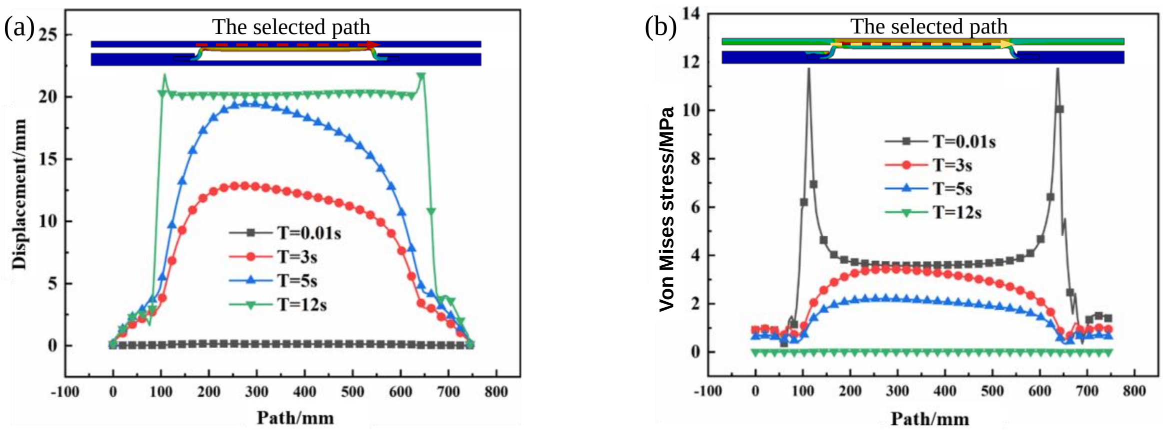

Figure 9. Displacement and Mises stress along a specific path in the rubber cylinder under different setting times: (a) displacement and (b) von-Mises stress

3.2 Fluid-Structure Coupling on the Setting Performance

Figure 10 shows the variation in flow velocity and pressure during the setting process. The flow velocity in the middle section of the basin gradually increases as setting time increases, reaching a maximum of 57.9 m/s at t = 5 seconds. According to continuity, expanding the rubber cylinder reduces the fluid's area in the annulus, leading to an increase in flow velocity. When t = 0.01seconds and t = 3 seconds, the pressure change inside the fluid area is quite small.

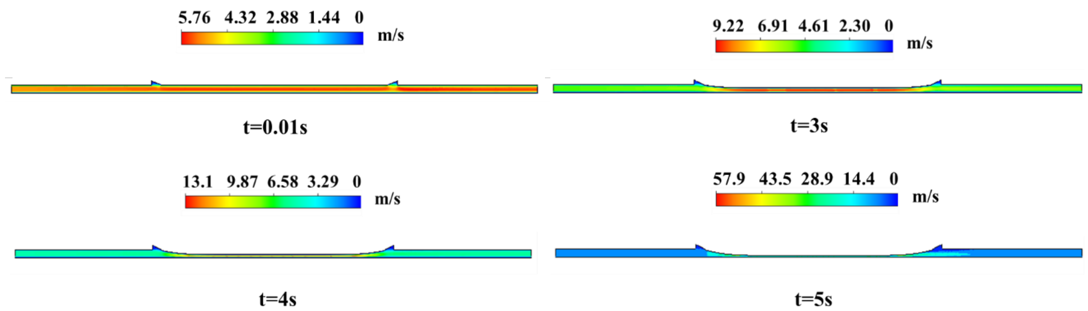

(a) Flow velocity

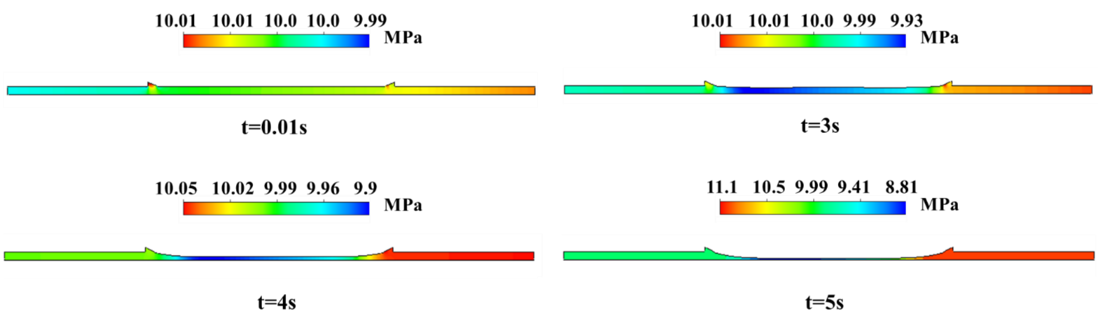

(b) Pressure

Figure 10. Flow velocity and pressure variation during the sealing process: (a) velocity and (b) pressure

However, when the annulus is sealed off at t =5seconds, the pressure difference in the fluid area is very apparent. The fluid pressure is significantly impacted by the velocity gradient of the liquid. As the annular area gradually decreases during the setting process, the velocity gradient at the front end of the sealing area increases, resulting in an increase in the fluid pressure and setting difficulty.

The contact area and contact stress on the sealing cylinder are the primary determinants when evaluating the sealing efficacy of the downhole emergency packer. Several fluid factors can influence the setting effect, such as flow velocity and intake pressure. Figure 11 shows the average contact area and contact stress of the rubber cylinder under different flow velocities (the inlet pressure is maintained at 10 MPa). The average contact area is the area obtained by integrating the contact stress curve. The average contact stress is 11.15 MPa when the inlet fluid velocity is 5 m/s. As the inlet fluid velocity increases, the contact area and average contact stress continue to decrease. As a result, the sealing properties can be significantly weakened when the flow of inlet fluid is considered.

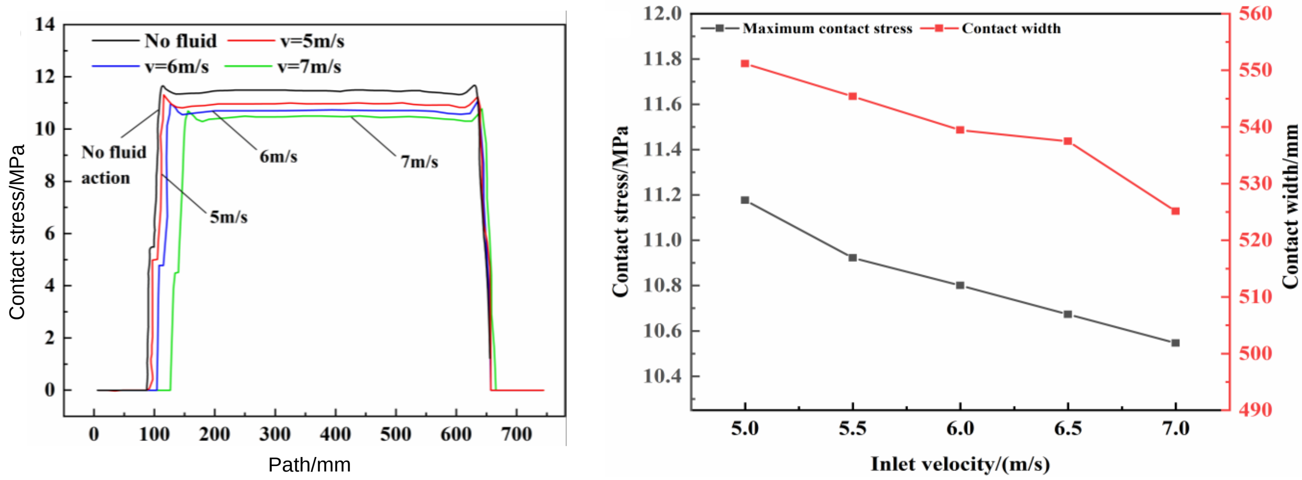

Figure 11. The influence of fluid velocity on setting performance: (a) contact stress variation along contact and (b) maximum contact stress and contact width versus inlet velocity

To provide a more accurate evaluation of the sealing properties, the sealing coefficient, K with the following expression was used to evaluate the sealing properties of the rubber cylinder,

$$K = C_P \times C_L \tag{7}$$

where, C_P is the contact stress and C_L is the contact length.

Figure 12 shows the variation of K with increasing fluid velocities. K reaches 6290.56 MPa. mm without the fluid action. However, it decreases with the increase in fluid velocity once the fluid acts on it. Assuming K_0 as the initial coefficient value without fluid action, K_1 is the sealing coefficient considering the fluid flow, the sealing loss, L caused by fluid interaction can be calculated as,

$$L = \frac{K_0 - K_1}{K_0} \times 100\% \tag{8}$$

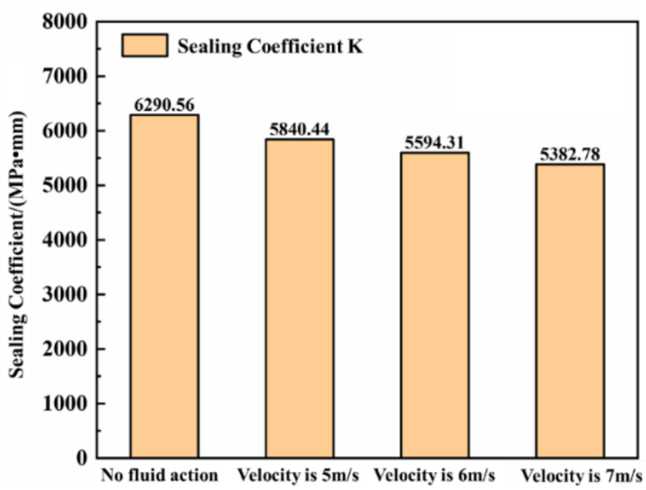

Figure 12. K at different fluid velocities (fluid pressure 10 MPa)

According to Eq. (8), the sealing losses, L at inlet flow rates of 5 m/s, 6 m/s, and 7 m/s are 7.15%, 11.06%, and 14.4%, respectively. The fluid-structure coupling method can provide a more accurate evaluation of the sealing properties of the rubber cylinder. At present, the setting pressure of a conventional packer is generally determined according to the size of the annulus and rubber cylinder, and the mechanical properties of the rubber. However, this design is insufficiently secure when dealing with downhole emergency conditions. The setting pressure of the emergency packer should be increased to ensure setting process effectively and safely.

4. CONCLUSIONS

In this work, the downhole emergency packer was designed to address the potential risks of kicks and high-pressure overflow during offshore drilling. A fluid-structure coupling model was established, and the fluid-structure interaction during the setting process was simulated to evaluate the influence of fluid flow on the setting pressure and setting effect. The primary findings are as follows:

i) The downhole emergency packer designed can achieve the setting function of the annular space between the 9 ⅝" casing and 5" drill pipe, effectively suppressing the well kick and high-pressure overflow moving up from the well bottom to the wellhead.

ii) According to the fluid-structure coupling model, the rubber cylinder's setting procedure can be divided into the extrusion step, contact deformation stage, and sealing completion stage. The rubber cylinder expands, decreasing the annulus area at the sealing section, resulting in a significant rise in fluid velocity and pressure between the intake and setting section, hence exacerbating sealing difficulties.

iii) The presence of fluid flow significantly reduces the sealing properties of the rubber cylinder. The sealing performance decreases with the increase in fluid velocity, and the sealing coefficient, K decreases by 7.15%, 11.06%, and 14.4% when the flow velocities from the inlet were 5 m/s, 6 m/s, and 7 m/s, respectively. Therefore, the setting pressure should be raised according to the actual downhole working conditions to achieve the actual setting effect safely.

ACKNOWLEDGEMENTS

The research work was supported by the National Key R&D Program of China (No. 2024YFC3014003), the National High Tech Ship Research Project (No.CBG2N21-4-2), and the National Natural Science Foundation of China (No. 52274026).

CONFLICT OF INTEREST

The authors declare no conflicts of interest.

AUTHORS CONTRIBUTION

L. C. Zhou (Investigation; Visualization; Writing-original draft)

W. J. Song (Conceptualization; Resources; Funding Acquisition)

H. H. Liu (Validation; Visualization)

X. G. Huang (Methodology; Writing-review & editing; Supervision)

AVAILABILITY OF DATA AND MATERIALS

The data supporting this study’s findings are available on request from the corresponding author.

ETHICS STATEMENT

Not applicable

REFERENCES

[1] M. Bai, A. Shen, L. Meng, J. Zhu, K. Song, “Well completion issues for underground gas storage in oil and gas reservoirs in China,” *Journal of Petroleum Science Engineering*, vol. 171, pp. 584-591, 2018.

[2] P. Wang, M. Cai, Z. Liu, W. Ma, J. Li, “Research on key technology of packer rubber barrel for integrated fracturing and completion of gas well,” *Journal of Petroleum Exploration Production Technology*, vol. 14, no. 3, pp. 825-838, 2024.

[3] R. S. Rivlin, “Large elastic deformations of isotropic materials IV: Further developments of the general theory,” *Philosophical Transactions of the Royal Society of London. Series A, Mathematical Physical Sciences*, vol. 241, no. 835, pp. 379-397, 1948.

[4] M. Mooney, “A theory of large elastic deformation,” *Journal of Applied Physics*, vol. 11, no. 9, pp. 582-592, 1940.

[5] O. H. Yeoh, “Some forms of the strain energy function for rubber,” *Rubber Chemistry Technology*, vol. 66, no. 5,

pp. 754-771, 1993.

[6] R. W. Ogden, “Large deformation isotropic elasticity–on the correlation of theory and experiment for incompressible rubberlike solids,” *Proceedings of the Royal Society of London. A. Mathematical Physical Sciences*, vol. 326, no. 1567, pp. 565-584, 1972.

[7] A. N. Gent, “A new constitutive relation for rubber,” *Rubber Chemistry and Technology*, vol. 69, no. 1, pp. 59-61, 1996.

[8] J. Cui, W. Qiu, S. Huang, T. Sun, Z. Lu, S. Wang, et al., “Mechanical property analysis, simulation and theoretical calculation of silicone rubber joint assembled in HV cable under certain circumstances,” in *2nd International Conference on Electrical Materials and Power Equipment (ICEMPE)*, pp. 361-367, 2019.

[9] T. Beda,"Modeling hyperelastic behavior of rubber: A novel invariant-based and a review of constitutive models," *Journal of Polymer Science Part B: Polymer Physics*, vol. 45, no. 13, pp. 1713-1732, 2007.

[10] V. Shim, L. Yang, C. Lim, P. Law, "A visco-hyperelastic constitutive model to characterize both tensile and compressive behavior of rubber," *Journal of Applied Polymer Science*, vol. 92, no. 1, pp. 523-531, 2004.

[11] Y. Liu, L. Qian, J. Zou, C. Xia, Z. Lian, “Study on failure mechanism and sealing performance optimization of compression packer,” *Engineering Failure Analysis*, vol. 136, p. 106176, 2022.

[12] X. Zheng, B. Li, G. Fei, “Evaluation of sealing performance of a compression packer at high temperature,” *Science Progress*, vol. 105, no. 1, p. 00368504221079180, 2022.

[13] Y. Liu, Z. Lian, J. Chen, S. Kuang, Y. Mou, Y. Wang, “Design and experimental research on sealing structure for a retrievable packer,” *Shock Vibration*, vol. 2020, no. 1, p. 7695276, 2020.

[14] P. Fan, Y. Kuang, B. Yang, “A new incremental calculated approach to predict maximum contact stress of compressed packer in large deformation,” *Proceedings of the Institution of Mechanical Engineers, Part C: Journal of Mechanical Engineering Science*, vol. 236, no. 6, pp. 2918-2930, 2022.

[15] Y. Kang, Z. Long, T. Kang, Z. Ren, T. Shi, X. Zhang, “Adaptability of hydraulic fracturing packers and optimization of their sealing performance for three common clastic rock reservoirs based on finite element analysis,” *Frontiers in Earth Science*, vol. 10, p. 986344, 2022.

[16] J. Liu, K. Deng, S. Liu, X. Yan, L. Li, D. Zou, et al., “Mechanical behavior and structure optimization of compressed PHP packer rubber,” *Journal of Materials Engineering Performance*, vol. 30, pp. 3691-3704, 2021.

[17] F. Zhang, X. Jiang, H. Wang, N. Song, J. Chen, J. Duan, “Mechanical analysis of sealing performance for compression packer rubber tube,” *Mechanics Industry*, vol. 19, no. 3, p. 309, 2018.

[18] X. Zheng, B. Li, “Study on sealing performance of packer rubber based on stress relaxation experiment,” *Engineering Failure Analysis*, vol. 129, p. 105692, 2021.

[19] B. Alcock, J. K. Jørgensen, “The mechanical properties of a model hydrogenated nitrile butadiene rubber (HNBR) following simulated sweet oil exposure at elevated temperature and pressure,” *Polymer Testing*, vol. 46, pp. 50-58, 2015.

[20] L. Dong, K. Li, X. Zhu, Z. Li, D. Zhang, Y. Pan, et al., “Study on high temperature sealing behavior of packer rubber tube based on thermal aging experiments,” *Engineering Failure Analysis*, vol. 108, p. 104321, 2020.

[21] L. Jin, Z. Xue, Z. Wang, R. Li, J. Liu, “Mechanical response of the sealing packer based on two rubber materials at high temperatures,” *Polymer Testing*, vol. 124, p. 108073, 2023.

[22] E. Burman, M. A. Fernández, S. Frei, F. M. Gerosa, “A mechanically consistent model for fluid–structure interactions with contact including seepage,” *Computer Methods in Applied Mechanics Engineering*, vol. 392, p. 114637, 2022.

[23] J. Wu, L. Li, “Influence of ambient pressure on sealing performance of O-ring in deep-sea hydraulic system,” *Ocean Engineering*, vol. 245, p. 110440, 2022.

[24] B. Yang, R. Salant, “Elastohydrodynamic lubrication simulation of O-ring and U-cup hydraulic seals,” *Proceedings of the Institution of Mechanical Engineers, Part J: Journal of Engineering Tribology*, vol. 225, no. 7, pp. 603-610, 2011.

[25] C. Wen, A. Yang, L. Tseng, W. Tsai, “Flow analysis of a ribbed helix lip seal with consideration of fluid–structure interaction,” *Computers fluids*, vol. 40, no. 1, pp. 324-332, 2011.

[26] Y. Ran, Q. He, W. Huang, Y. Liu, Y. Wang, “Analysis of the coupling mechanism of the dynamic response and mechanical-thermal deformation in mechanical seals,” *Tribology International*, vol. 192, p. 109257, 2024.

[27] C. Xiang, F. Guo, X. Liu, Y. Chen, X. Jia, Y. Wang, “Numerical algorithm for fluid–solid coupling in reciprocating rod seals,” *Tribology International*, vol. 143, p. 106078, 2020.

[28] J. Wei, Y. Xue, J. Tian, F. Guo, “Study on the prediction of high-speed rotary lip seal wear in aero-engine based on heat-fluid-solid coupling,” *Industrial Lubrication Tribology*, vol. 76, no. 2, pp. 167-177, 2024.

[29] J. Angerhausen, H. Murrenhoff, B. N. Persson, L. Dorogin, M. Scaraggi, "Finite element based transient elastohydrodynamic simulation of translational hydraulic seals," *International Journal of Fluid Power*, pp. 1-26, 2019.

[30] J. Yan, Z. Zhang, J. Man, J. Sun, R. Zhen, X.-a. Liu, "Parameter Identification of the Mooney–Rivlin Model for Rubber Mounts Subject to Multiaxial Load," *Journal of Vibration Engineering Technologies*, vol. 13, no. 1, pp. 1-17, 2025.

[31] G. Hu, P. Zhang, G. Wang, M. Zhang, M. Li, "The influence of rubber material on sealing performance of packing element in compression packer," *Journal of Natural Gas Science Engineering*, vol. 38, pp. 120-138, 2017.

[32] S. Hwang, A. Khayyer, H. Gotoh, J. Park, "Development of a fully Lagrangian MPS-based coupled method for simulation of fluid–structure interaction problems," *Journal of Fluids Structures*, vol. 50, pp. 497-511, 2014.

[33] J. Hu, X. Ning, S. Sun, F. Li, J. Ma, W. Zhang, "Fluid-structure coupled analysis of flow-induced vibrations in three dimensional elastic hydrofoils," *Marine Structures*, vol. 84, p. 103220, 2022.

[34] G. Hu, M. Wang, G. Wang, T. Zhu, L. Wei, "Sealing performance and failure mechanism analysis of packing unit used in rotary blowout preventer for under-balanced drilling," *Engineering Failure Analysis*, vol. 129, p. 105654, 2021.

[35] G. Hu, G. Wang, M. Li, X. He, W. Wu, "Study on sealing capacity of packing element in compression packer," *Journal of the Brazilian Society of Mechanical Sciences Engineering*, vol. 40, pp. 1-9, 2018.